

Selective Removal of La(III) Ions Using Super-Paramagnetic Nanosorbent Coated by Saponified *sec*-Octylphenoxy Acetic Acid

Baohui Zhu,[†] Dongbei Wu,^{*,†} Yuhui Yang,[†] Yonggui Chen,^{‡,§} Wenjun Li,[†] Junfang Guo,^{||} and Qigang Wang[†]

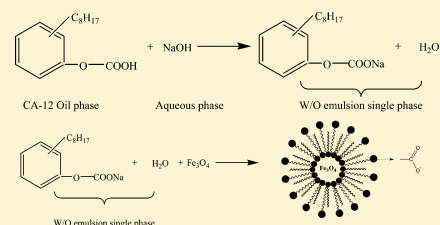
[†]Department of Chemistry, Tongji University, 1239 Siping Road, Shanghai, P. R. China 200092

[‡]Key Laboratory of Geotechnical & Underground Engineering of Ministry of Education, Tongji University, 1239 Siping Road, Shanghai 200092, P. R. China

[§]Department of Geotechnical Engineering, Tongji University, 1239 Siping Road, Shanghai, P. R. China 200092

^{||}School of Material Science and Engineering, Wuhan Institute of Technology, 430073, Wuhan, P. R. China

ABSTRACT: Super paramagnetic nanosorbents coated by saponified *sec*-octylphenoxy acetic acid (MSCA-12) were prepared as a kind of sorbent for magnetically assisted chemical separation of lanthanum(III) ions using an equilibrium batch experiment. The effects of various parameters such as contact time, pH, ion strength, interference ions, and metal ion concentration on the adsorption was investigated. The optimal pH for La(III) ions was equilibrium pH 7.0. The adsorption isotherm followed the Langmuir model with the maximum sorption capacity of 22.0 mg·g⁻¹. The sorbent showed a good affinity toward La(III), and the stability of the sorbent in acidic solutions was also improved by the coating. The recovery of La(III) could be achieved using a 0.01 mol·kg⁻¹ HCl solution. The repeated use three times of the adsorbent was possible. The sorbent was shown to have potential in the extraction of La(III) from the lake water, ground waters, and artificial wastewater.



1. INTRODUCTION

Rare earth elements have received considerable attention with increasing demands in hi-tech industries for their unusual spectroscopic characteristics. A future growth area for rare earth elements is in rechargeable batteries, fiber optics, scintillation detectors, medical isotopes, and surgical lasers. Lanthanum, one of the most abundant rare earth elements, is of current interest and usually applied in advanced new materials such as superalloys, catalysts, special ceramics, and organic synthesis.¹ Though rare earth elements do not represent a common toxic threat, it can be forecasted that the introduction of so many rare earth ions into the environment through various pathways will finally result in environmental problems in the next few decades.² Therefore, the need for an effective and economical process to remove rare earth ions from aqueous solution has drawn much attention. The removal of rare earth ions can be achieved by several processes, chemical precipitation, adsorption, or solvent extraction; each one has its own advantages and limitations in application.

The magnetically assisted chemical separation (MACS) method was first developed by Palyska and Chmielewski for the extraction of Cu²⁺ (with D-2EHPA) and UO₂²⁺ (with TBP) ions from aqueous media in magnetic field experiments.³ After that, Argonne National Laboratory (ANL) carried out a lot of research work and opened a new site for the separation and removal of metal ions,⁴ radionuclide and transuranic elements,^{5,6} and organic compounds.⁷ The MACS method combines the selective and efficient separation offered by

chemical extraction with the magnetic removal of extractant for object ions or compounds.⁸ The greatest advantage of this method is that the separation in magnetic field allows better separation and the reduced size of equipment. The stability and selectivity of bare magnetic particles in strong acidic solutions was also improved when coated. Currently, the main method that has been used for coating the extractant onto the surface of the magnetic particles is physical adsorption. The lipophilic extractant was directly coated onto the surface of the hydrophilic iron oxide core by vigorous stirring. It was observed that the uptake mass fraction of extractant was approximately to be 0.05, which resulted in a low adsorption efficiency.⁹ On the other hand, the used magnetic microparticle was not super-paramagnetic. When the external magnet field disappeared, the sorbent had a residual magnetism, which was adverse to adsorption and removal of the metal ions from the aqueous solutions.

Therefore, in this work, we try to develop a modified physical adsorption method for the preparation of super-paramagnetic nanoadsorbent coated by the extractant and then used for selective removal of lanthanum from aqueous solutions. First, the extractant *sec*-octylphenoxy acetic acid (abbreviated as CA-12) was saponified to be sodium carboxylate–water emulsion by reacting with concentrated sodium hydroxide, and then, the

Received: October 19, 2011

Accepted: December 13, 2011

Published: December 22, 2011

super paramagnetic iron oxide nanoparticles were synthesized by the coprecipitation method; finally, the super-paramagnetic nanoadsorbent was assembled by physical adsorption of saponified CA-12 onto the surface of the as-prepared magnetic nanoparticle. The CA-12 was saponified and preferred due to its high separation factor toward La(III) ions¹⁰ and an excellent affinity toward hydrophilic Fe₃O₄ core after saponification. Though there were a few reports on the separating metal ions using extractant-coated magnetic particles as a magnetic sorbent, however, the information on the removal of rare earth ions was not available. For this presentation, a scanning electron microscope (SEM), wide-angle X-ray diffraction (WXR), Fourier transform infrared spectra (FT-IR), and a vibrating sample magnetometer (VSM) were used for the characterization of magnetic sorbent. Various effects of contact time, ionic strength, pH, interference ions, and metal ion concentration on the extraction were investigated. Finally, the model wastewater and the lake and groundwater spiked with La(III) were prepared for removal of lanthanum at optimal experimental conditions.

2. EXPERIMENTAL SECTION

2.1. Reagents. Stock solution of lanthanum was prepared from its oxides via dissolution in concentrated hydrochloric acid and standardized by ethylenediamine tetraacetic acid (EDTA) titration with xylenol orange as the indicator. *sec*-Octylphenoxy acetic acid (CA-12, mass fraction is 0.93, Laiyashi Chemical Company in Shanghai, P. R. China) was used as an extractant and diluted with kerosene. Ferric chloride hexahydrate, ferrous chloride tetrahydrate, ammonia, and other reagents were of analytical grade from China. The pH of the solutions was adjusted to the required value with 0.01 mol·kg⁻¹ HCl and 0.01 mol·kg⁻¹ NaOH solutions.

2.2. Apparatus. A UV–vis spectrophotometer (China, model UV-752) and an inductively coupled plasma atomic emission spectrometer (ICP-AES) IRIS Advantage 1000 from Thermal Elemental USA were used for the determination of metal ions. A Mettler Toledo FiveEasy digital Orion pH meter was used for pH adjustment. A Nicolet FT-IR 560 Magna spectrometer using KBr (neat) was used to obtain the infrared spectra of the coated magnetic particles. A scanning electron microscope (SEM: JEOL, JSM-5410 LV) was used to observe the surface morphology. X-ray diffraction (XRD) was done in a diffractometer (model APD-10, Philips, Netherlands) equipped with Cu K $\alpha_{1,2}$ radiation source between 10° and 70° (2 θ) at room temperature. The magnetization curve of the magnetic particles was recorded with a vibrating sample magnetometer (USA, model Lakeshore 7400) for a solid sample at room temperature with an applied magnetic field up to 7000 Oe.

2.3. Preparation of Magnetic Nanoadsorbent. There are three steps to prepare the magnetic nanoadsorbent: (i) CA-12 was saponified to be sodium carboxyl–water emulsion by adding a stoichiometric amount of a concentrated NaOH solution to the extractant in kerosene and stirring the mixture for 48 h to form a W/O single phase. This W/O emulsion had a high interfacial activity,¹¹ which should exhibit a high affinity toward hydrophilic Fe₃O₄ core. The saponification percentage was determined by using the titration method with NaOH solution. In the solid–liquid extraction experiments with the saponified CA-12 modified magnetic nanoparticles, the mole fraction of the saponification was kept at 0.65. (ii) Super-paramagnetic iron oxide nanoparticles were prepared by the coprecipitation method. The details and the advantages of the

method were described in an earlier research work.^{12,13} (iii) The solvent evaporation method was used for the preparation of magnetic nanoadsorbent. Simply, a known weight of magnetic particles (2.0 g) was ultrasonically mixed with saponified CA-12 emulsion (50 mL) for 1 h, and then the resultant material was separated with an external magnet; after solvent evaporation by blasting N₂ for two days, the magnetic particles were finally vacuum-dried to a constant weight prior to use. The content of sodium ion in the magnetic sorbent was determined to be 2.74 mmol·g⁻¹ by atomic absorption spectroscopy (AAS). The mass fraction of the saponified CA-12 loaded on the magnetic nanoparticles was calculated to be 0.169 by mass balance. According to our four parallel experiments by adjusting the mass/volume ratio of magnetic nanoparticle and CA-12, this value is the biggest of all. The formation of super-paramagnetic nanoadsorbent (MSCA-12) can be drawn as Figure 1. Similarly to the above procedure, the

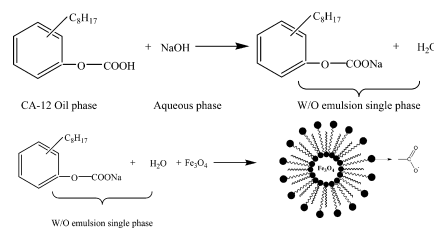


Figure 1. Formation of saponified CA-12 magnetic nanoparticles.

unsaponified CA-12 nanoparticles (abbreviated as UMSCA-12) were prepared, and the mass fraction of the CA-12 was about 0.06. The amount of the CA-12 coated onto the surface of magnetic nanoparticles was obviously improved by the saponification.

2.4. Solid–Liquid Extraction Procedure. Solid–liquid extraction experiments were performed by a mechanical shaker at 200 rpm with 30 mg of dry magnetic sorbent in contact with 30 mL of LaCl₃ solution (concentration ranges from (0.6 to 140) mg·kg⁻¹) at varying pH from 2.0 to 10.0 for 60 min at 298 K. It was confirmed through the preliminary experiments that 60 min was sufficient to attain equilibrium between sorbent and adsorbate. Before extraction, the solution pH was adjusted by using 0.01 mol·kg⁻¹ HCl and 0.01 mol·kg⁻¹ NaOH. No additional sodium chloride was added except for the study of the effect of ionic strength on the adsorption. After attaining equilibrium, the sorbent was separated by an external magnet, and MSCA-12-La nanoparticles were collected. The residual metal concentration in the supernatant was directly determined using a UV–vis spectrophotometer with arsenazo(III) as a colorimetric reagent. The amount of adsorbed metal ions was calculated by the material balance of the initial and equilibrium concentrations of the solution. The amount adsorbed per unit mass of adsorbent at equilibrium was given as follows

$$q_e = (C_{in} - C_e)V/m \quad (1)$$

where C_{in} and C_e (mol·kg⁻¹) denotes the initial and equilibrium concentrations of the La(III) ion in aqueous solution, respectively, V is the total volume of the solution in liters, and m is the mass of the dry magnetic adsorbent used in grams.

Consecutive adsorption–desorption cycles were repeated five times using the same magnetic adsorbent. In each cycle, 0.72 mg of La(III) in 30 mL of solution was mixed with 50 mg of MSCA-12 for 60 min. MSCA-12 was separated, and the

supernatant composed of lanthanum and iron was subjected to measurements. The resultant La-loaded sorbent was mixed with 10 mL of 0.01 mol·kg⁻¹ HCl solution for 60 min. Prior to the next adsorption–desorption cycle, regenerated MSCA-12 was washed thoroughly with distilled water until pH 6.2.

2.5. Removal of La(III) from Lake and Ground Waters. Ground water was collected from the Tongji University area in the middle of Shanghai, P. R. China. Lake water was collected from Shang Lake, Changshu in the Jiangsu Province of P. R. China. The samples were used without any filtration. The concentration of metal ions in water samples was determined by ICP-AES. The accuracy of the method was evaluated by spiking 1.7 μg·kg⁻¹ of La(III) in contact with 50 mg of adsorbent to 100 mL of sample volume (three replicates).

2.6. Removal of La(III) from Model Wastewater. A model waste solution (100 mL) was brought in contact with 50 mg magnetic adsorbent at pH 7.0 at room temperature for 60 min. Model wastewater was prepared with a composition of 0.72 mg of La(III), 0.72 mg of each rare earth ion compound containing NdCl₃ and YbCl₃, 7.2 mg of each transition metal ion compound including ZnSO₄, CdCl₂, NiCl₂, and CoSO₄, 72 mg of each alkyl earth ion compound containing MgCl₂ and BaCl₂, and 720 mg of each alkaline ion compound (NaCl, KNO₃, LiAc); no precipitate was found at pH 7.0. After extraction, the concentration of metal ions in the supernatant was determined by ICP-AES.

3. RESULTS AND DISCUSSION

3.1. Characterization of the Sorbent. FTIR spectra of pure Fe₃O₄ and MSCA-12 before and after La(III) adsorption are compared in Figure 2. Absorption peaks at 628 cm⁻¹ and

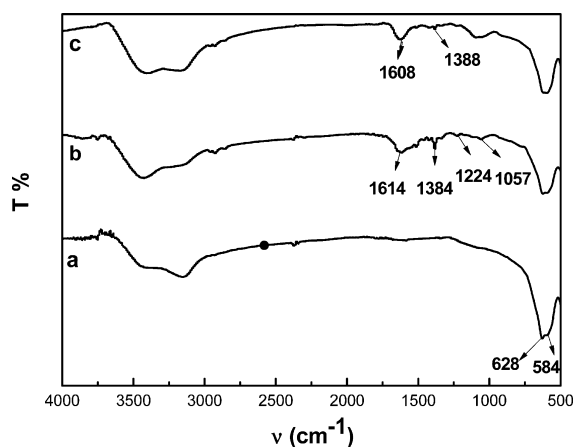


Figure 2. FTIR of pure Fe₃O₄ and MSCA-12 before and after La(III) adsorption. a: Fe₃O₄; b: MSCA-12; c: MSCA-12-La.

584 cm⁻¹ were observed, corresponding to the Fe–O vibration from the magnetite phase.¹⁴ The absorption bands at 1614 cm⁻¹ (strong asymmetrical stretching vibration bond (–C=O) in carboxyl groups), 1381 cm⁻¹ (weak symmetrical stretching vibration bond (–C–O) in carboxyl groups), 1224 cm⁻¹ (the –C=C–O stretching of vinethene groups), and 1057 cm⁻¹ (–C–O stretching of alcoholic groups) observed on MSCA-12 indicated the coating of saponified CA-12 on the magnetite surface.¹⁵ After La(III) adsorption, the adsorption peak at 1614 cm⁻¹ and 1384 cm⁻¹ shift to 1608 cm⁻¹ and 1388 cm⁻¹,

respectively, indicating that the –COO⁻ group in CA-12 contributes to the adsorption.

The crystalline structures of the nanoparticles are identified with XRD (Figure 3). For Fe₃O₄, diffraction peaks with 2θ at

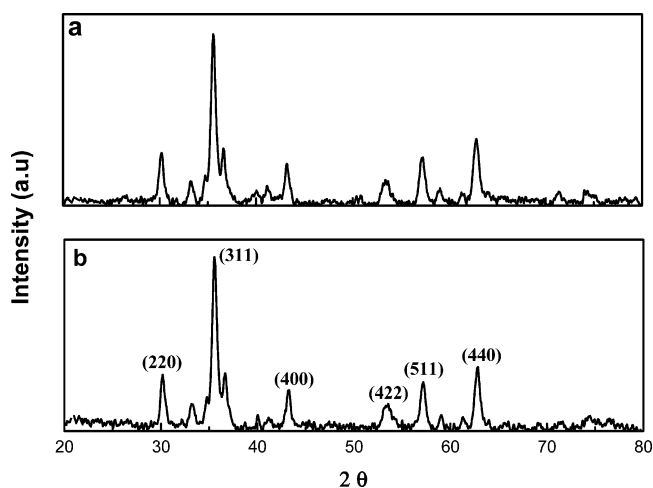


Figure 3. Powder XRD patterns of Fe₃O₄ and MSCA-12. (a) Fe₃O₄; (b) MSCA-12.

30.1°, 35.5°, 43.1°, 53.4°, 53.4°, and 62.6° were observed, indicative of a cubic spinel structure of the magnetite.¹⁶ The same sets of characteristic peaks were also found for MSCA-12, suggesting the stability of the crystalline phase of Fe₃O₄ nanoparticles when coated. The particle sizes of the magnetite calculated using the Scherrer equation were 9.1 nm and 9.3 nm for Fe₃O₄ and MSCA-12, respectively.

The magnetization curves measured for Fe₃O₄ and MSCA-12 before and after La(III) extraction are compared in Figure 4.

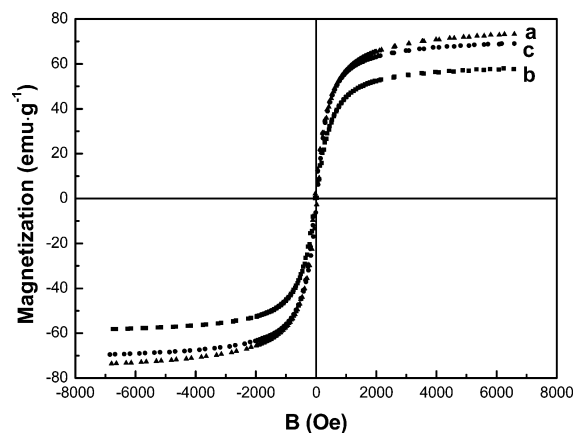


Figure 4. Magnetization curves of Fe₃O₄, MSCA-12, and MSCA-12-La. a: Fe₃O₄; b: MSCA-12; c: MSCA-12-La.

There was no hysteresis in the magnetization for three tested nanoparticles. Neither coercivity nor remanence was observed, suggesting that three nanoparticles were super-paramagnetic. The saturation magnetization (M_S) value was measured to be 73.4 emu·g⁻¹ for Fe₃O₄, 58.0 emu·g⁻¹ for MSCA-12, and 69.3 emu·g⁻¹ for MSCA-12-La, respectively. Although the saturation magnetization decreased when coated, complete magnetic separation of MSCA-12 samples was achieved in 2 min by placing a magnet near the vessels containing the aqueous dispersion of the nanosorbent. Especially, after La(III)

adsorption, the saturation magnetization increased again which might be owing to the strong magnetic field dependence of lanthanum ions.

The morphologies of the bare magnetic nanoparticles and MSCA-12 are illustrated in Figure 5. The bare magnetic

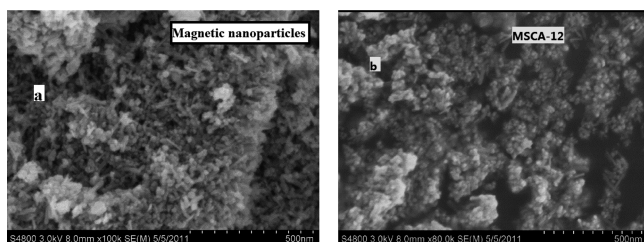


Figure 5. SEM images of (a) magnetic nanoparticles and (b) MSCA-12.

nanoparticles and MSCS-12 showed the agglomerate in various sizes, but the outer surface of MSCA-12 appeared to be smoother than the bare magnetic nanoparticles, indicating a kind of protection brought by the coating.

3.2. Stability of MSCA-12 in the Acidic Solution. The dissolution of magnetic particles could limit the use of the particles as adsorbents. Therefore, the leaching of Fe from the bare magnetic particles and MSCA-12 was studied. The amount of dissolved Fe was determined by AAS. A significant dissolution of the bare magnetic particles was found in strong acidic solutions ($\text{pH} < 3$). At $\text{pH} 1.0$, most of iron oxide was dissolved while less than 0.01 in mass fraction leaching extent from MSCA-12 was observed. The coating resulted in a better acid resistance property of magnetic adsorbent. Nevertheless, the observed leaching of Fe from the coated adsorbent in strong solution indicates that the surface of the adsorbent was not completely protected.

3.3. Effect of pH on Metal Extraction. The effect of pH on the extraction of La(III) ions from chloride medium was studied, and the results are shown in Figure 6a. It was clearly demonstrated that the extraction was strongly affected by pH. The maximum of extraction were obtained at equilibrium pH 7.0 for MSCA-12, and the value rapidly decreased with increasing pH. Since the La(III) ions are easy to coordinate with water molecules, a speciation diagram that accounts for La:OH 1:1, 1:2, 1:3, 2:2, 2:3, 2:5, 5:9, and 5:10 soluble species and the K_{sp} associated with the 1:3 species should be attached according to the values of stability constants of La(III) complexes (not be shown).¹⁷ The speciation diagram is identical for lanthanum ranging from $0.01 \text{ mmol}\cdot\text{kg}^{-1}$ to $10 \text{ mmol}\cdot\text{kg}^{-1}$. At $0.1 \text{ mol}\cdot\text{kg}^{-1}$ La, the 1:3 solid precipitates appreciably. Starting at just over pH 6, free lanthanum is no longer the predominant species. The predominant species is now the $\text{La}(\text{OH})_2^+$ species. Though the acetic acid can also coordinate with the La(III) ions, it is understood that the acetic acid cannot take part in the extraction because the acetic acid does not compete sufficiently with the lanthanum hydrolysis. In strong acidic solutions, the adsorbent showed low adsorption capacity, probably due to the competitive adsorption between H^+ and La(III). Aqueous H^+ ions with higher concentration and smaller ionic radii were easier to be adsorbed onto the MSCA-12 than La(III) ions; with increasing pH, the concentration of aqueous H^+ became to decrease slowly, and the main component of La(III) changed to be $\text{La}(\text{OH})_2^+$; ion exchange between H^+ in carboxyl groups of MSCA-12 and

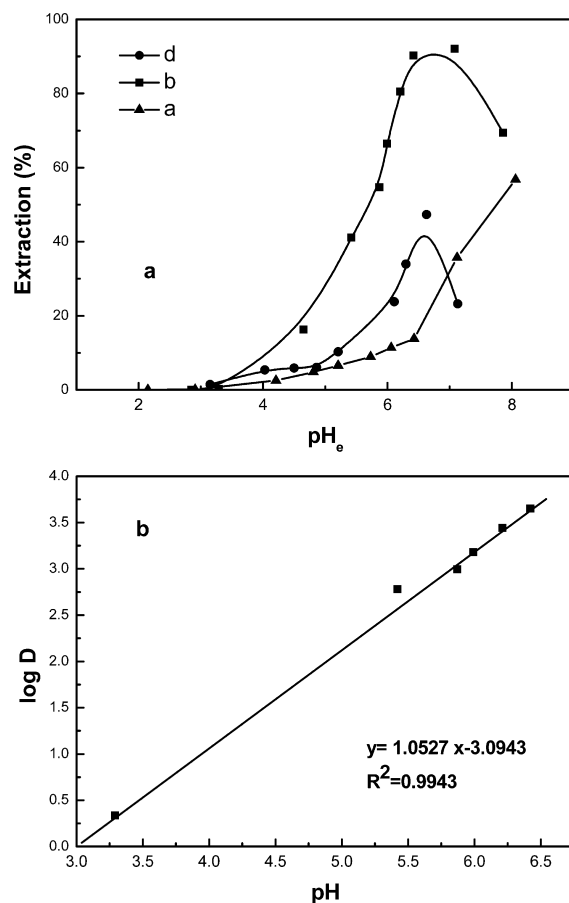


Figure 6. (a) Effect of pH on the adsorption. (b) Plot of $\log D$ vs pH. $C_{\text{ini}} = 24.6 \text{ mg}\cdot\text{kg}^{-1}$, $m = 30 \text{ mg}$, volume = 30 mL, contact time = 60 min. a: Fe_3O_4 ; b: MSCA-12; d: UMSCA-12.

aqueous $\text{La}(\text{OH})_2^+$ became predominant, and as a consequence, the extraction efficiency of La(III) increases, and the value of equilibrium pH decreases. By plotting $\log D$ against pH, the straight line with a slope of 1.0 could be obtained, suggesting that the adsorption performed the ion exchange mechanism (Figure 6b); after pH 7.0, the adsorption sharply decreased, which might be due to the precipitation and further hydrolysis of La(III) at the alkyl solution. Therefore, the pH value of La(III) solution used for subsequent experiments was 7.0. Also, it could be seen that the extraction percentage of MSCA-12 was higher than that of UMSCA-12 at the same pH, indicating an excellent adsorption efficiency of magnetic sorbent after saponification. The adsorption of La(III) with bare iron oxide was performed at the same conditions. The result demonstrated that the adsorption capacity of bare iron oxide was far lower than that of UMSCA-12 and MSCA-12 at $\text{pH} < 6.5$. A reasonable explanation is that, at $\text{pH} < 6.5$, the iron oxide particles carrying positive charges have a negative effect on the La(III) extraction. It was reported that the value of pHz of iron oxide nanoparticle by coprecipitation method was around 7.0.¹⁸ Almost no extraction at pH 2.0 exhibited that elution could be performed by a $0.01 \text{ mol}\cdot\text{kg}^{-1}$ HCl solution.

3.4. Effect of Extraction Time. The extraction time was varied from (2 to 70) min and the results are shown in Figure 7a. The maximum uptake of La(III) was achieved within 10 min and extraction fraction was 0.919. Therefore, for subsequent batch experiments, equilibrium time of 60 min

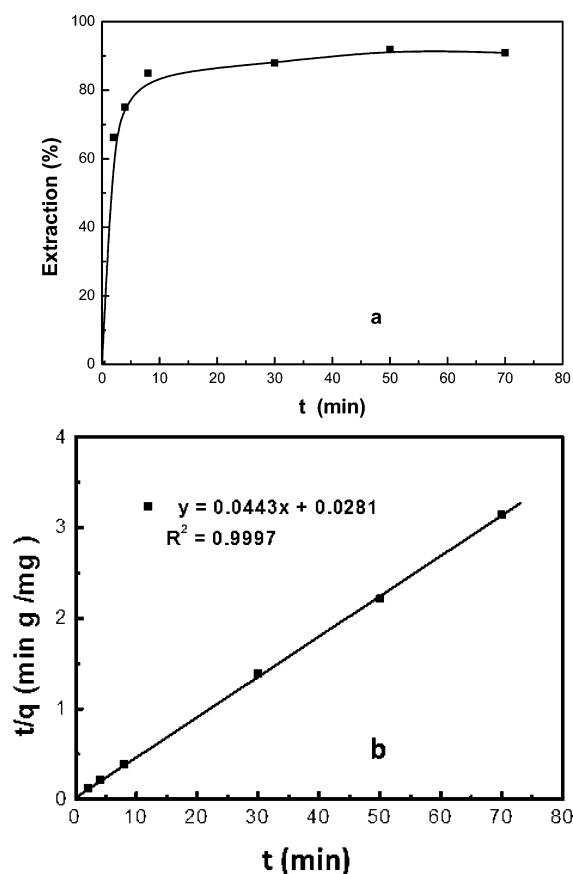


Figure 7. (a) Effect of time on the adsorption. (b) Plot of t/q against time. $C_{\text{ini}} = 24.6 \text{ mg}\cdot\text{kg}^{-1}$, $m = 30 \text{ mg}$, volume = 30 mL, pH = 7.0.

was sufficient to establish equilibrium and suitable for an application in the removal of trace metal ions.

The pseudosecond-order equation is often successfully used to describe the kinetics of the adsorption process. Its expression is as follows:

$$\frac{t}{q_t} = \frac{1}{k_2 q_e^2} + \frac{t}{q_e} \quad (2)$$

where k_2 ($\text{g}\cdot\text{mg}^{-1}\cdot\text{min}^{-1}$) is the second-order rate constant and q_t ($\text{mg}\cdot\text{g}^{-1}$) denotes the amount of La(III) adsorbed at any time t (min). By plotting t/q_t versus t , a straight line is obtained with the slope of $1/k_2 q_e^2$ and intercept of $1/q_e$ (Figure 7b). The calculated values of k_2 and q_e were $22.6 \pm 0.03 \text{ mg}\cdot\text{g}^{-1}$ and $0.070 \text{ g}\cdot\text{mg}^{-1}\cdot\text{min}^{-1}$, respectively. A high correlation coefficient indicates the applicability of the pseudosecond-order model, and adsorption follows the chemisorption mechanism.

Pseudofirst-order and intraparticle diffusion models were also used to describe the kinetics of the adsorption process. The lower correlation coefficients ($R^2 < 0.90$) indicated that they were not suitable for explanation of adsorption mechanism (not shown).

3.5. Effect of Ionic Strength. The effect of ionic strength on the extraction was studied in the potassium chloride solution and sodium chloride with various concentrations from (0 to 2.0) $\text{mol}\cdot\text{kg}^{-1}$. Results are shown in Table 1. Quantitative separation of La(III) was obtained in the concentration range of (0 to 0.02) $\text{mol}\cdot\text{kg}^{-1}$ KCl. The extraction fraction was 0.808 even in 2.0 $\text{mol}\cdot\text{kg}^{-1}$ saline solution. These observations showed the specific tendency of MSCA-12 for La(III) ions

Table 1. Effect of Ionic Strength on the Adsorption^a

C_{KCl} $\text{mol}\cdot\text{kg}^{-1}$	RF	C_{NaCl} $\text{mol}\cdot\text{kg}^{-1}$	RF
0	0.929 ± 0.01	0	0.933 ± 0.01
0.02	0.927 ± 0.03	0.02	0.905 ± 0.02
0.1	0.852 ± 0.03	0.1	0.857 ± 0.04
0.2	0.862 ± 0.05	0.2	0.797 ± 0.03
0.5	0.778 ± 0.04	0.5	0.809 ± 0.06
1.0	0.794 ± 0.04	1.0	0.783 ± 0.06
2.0	0.801 ± 0.08	2.0	0.806 ± 0.13

^aRF: removal fraction.

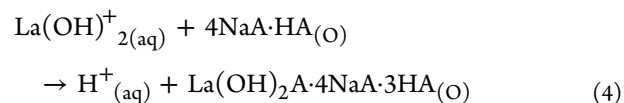
versus potassium ions and sodium ions and the possibility to separate La(III) from high saline solutions.

3.6. Adsorption Isotherm. The initial concentration provides an important driving force to overcome all mass transfer resistances of metal ions between the aqueous and solid phases. Hence a higher initial concentration of La(III) will enhance the adsorption process. The Langmuir isotherm assumes a surface with homogeneous binding sites and no interaction between adsorbed species. Its mathematical form can be written as:

$$\frac{C_e}{q_e} = \frac{C_e}{q_{\text{max}}} + \frac{1}{b q_{\text{max}}} \quad (3)$$

where q_{max} is the maximum amount of metal ions and b is the Langmuir parameter relates the affinity of the sorbate for the binding sites expressed in $\text{L}\cdot\text{mg}^{-1}$. q_{max} and b can be determined from the linear plot of C_e/q_e versus C_e .

Figure 8a shows the effect of metal ion concentration on the adsorption. As seen, the amount of La(III) ions adsorbed per unit mass of the MSCA-12 increased linearly with the equilibrium concentration of La(III) from (0.6 to 4.4) $\text{mg}\cdot\text{kg}^{-1}$ and reached a plateau in the adsorption profile at $24.6 \text{ mg}\cdot\text{kg}^{-1}$. According to the Langmuir model, the q_{max} was calculated to be $21.74 \pm 0.02 \text{ mg}\cdot\text{g}^{-1}$. The mole ratio of La(III) to MSCA-12 was 1:4 considering the maximum extraction capacity of the MSCA-12. This result had a good consistency with previous work reported by Wang et al.; that is, the stoichiometry of rare earth ions with *sec*-nonylphenoxy acetic acid complexes was 1:4.¹⁹ Therefore, the extraction could be deduced as eq 4:



where (aq) and (O) denote the aqueous and organic phase, respectively, and NaA·HA represents the saponified CA-12. Though magnetic nanoparticles could also adsorb some La(III) ions through the electrostatic interaction, a low adsorption capacity around $3.5 \text{ mg}\cdot\text{g}^{-1}$ at pH 7.0 indicated that the adsorption could be ignored. Furthermore, though it would have been very helpful to compare the adsorption capacity reported in this work to those in the literature, to our knowledge, such information was not available. Therefore, it is difficult for us to compare the superiority of this adsorbent to other similar adsorbents. However, Sert et al. reported that the adsorption capacity of *Platanus orientalis* leaf powder for lanthanum was $28.65 \text{ mg}\cdot\text{g}^{-1}$.¹ The maximum biosorption capacity of tap bentonite for lanthanum chloride of $17.85 \text{ mg}\cdot\text{g}^{-1}$ at 323 K was investigated by Chegrouche et al.²⁰ The

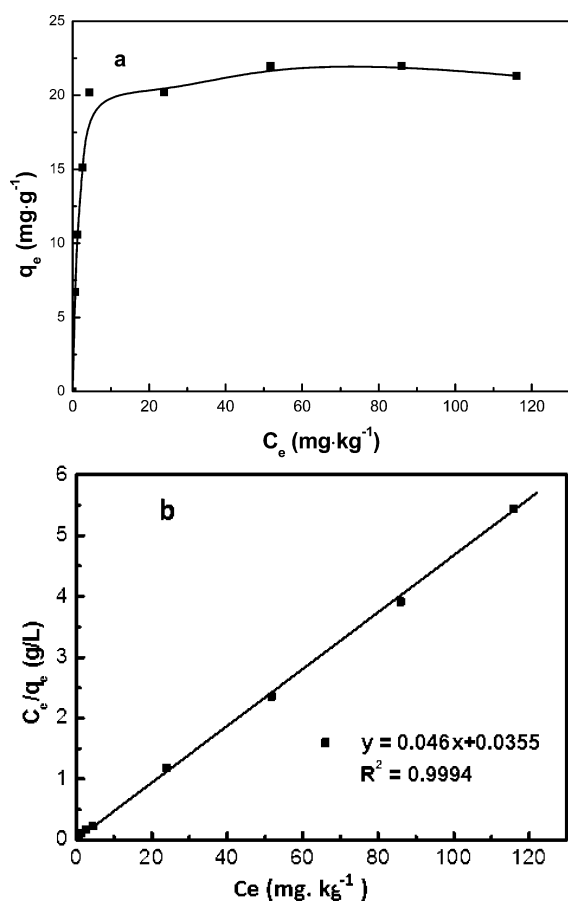


Figure 8. (a) Adsorption isotherm. (b) Plot of C_e/q_e versus C_e . $m = 30$ mg, volume = 30 mL, pH = 7.0, contact time = 60 min.

removal of lanthanum from nitrate medium using Aliquat-336 impregnated onto Amberlite XAD-4 was studied by Sofany, and the result demonstrated that the uptake capacity was $4.73 \text{ mg}\cdot\text{g}^{-1}$.²¹ Thus the adsorption capacity value reported in the present study is comparable to the above values reported in the literature.

Figure 8b indicates a better presentation of the Langmuir model with a high correlation coefficient of La(III) adsorption on the MSCA-12. The Langmuir parameter, b , can be used to predict the affinity between the sorbate and adsorbent using the dimensionless separation factor, R_L , and defined by Hall et al. as:

$$R_L = \frac{1}{1 + bC_{\text{ini}}} \quad (5)$$

where C_{ini} is the initial concentration of La(III) expressed in $\text{mg}\cdot\text{kg}^{-1}$ and b is the Langmuir adsorption equilibrium constant ($\text{kg}\cdot\text{mg}^{-1}$). If the value of R_L is equal to zero or one, the adsorption is either linear or irreversible, and if the value is in between zero and one, adsorption is favorable to chemisorption. The values of R_L changing from 0.05 to 0.006 in the range

of initial concentration from (0.6 to 140) $\text{mg}\cdot\text{kg}^{-1}$ imply the favorable chemisorption of La(III) by MSCA-12. Also, the Freundlich and Dubinin–Radushkevich (D–R) isotherm models were used for the description of adsorption process, and the lower correlations ($R^2 < 0.90$) indicated they were not suitable to explanation of adsorption mechanism (not be shown).

3.7. Desorption and Repeated Use. To examine the reusability of the prepared MSCA-12, sorption experiments (sorption–desorption cycle) were repeatedly performed using the same nanosorbents. A 30 mL portion of $0.01 \text{ mol}\cdot\text{kg}^{-1}$ HCl solution was used for the elution of La(III) ions and regeneration of the adsorbent. The sorption–desorption cycles were performed five times. Each experiment was performed under the following optimal conditions: initial metal ion concentration, $24 \text{ mg}\cdot\text{kg}^{-1}$; amount of MSCA-12, 50 mg; pH, 7.0; treatment period, 60 min. The results (Table 2) showed that MACA-12 could be repeatedly used three times with a slight loss in the initial binding affinity. After three adsorption–desorption cycles, the extraction efficiency of the adsorbents decreased obviously when reused. The reduction in adsorption efficiency might be attributed to the loss of the extractant resulting from the elution of active component. Besides that, the incomplete elution of the sorbed metal on the adsorbents was another possible reason. Therefore, the efficiency decreased each time when the adsorbents were reused. After five cycles of use, the extraction fraction decreased to 0.60 of the first cycle.

3.8. Effect of Interference Ions. In general, water contains ions other than La(III) with different concentrations depending on the source. These ions may affect the extraction efficiency of MSCA-12 due to the competition for the binding sites between La(III) ions and other ions. Certain ions also form a complex with La(III), resulting in insoluble compounds. The extraction efficiency of MSCA-12 was evaluated in the presence of interference ions (Table 3). There was no change in the efficiency of the extraction of La(III) ions in the presence of a hundred fold alkali metal ions (K^+ , Na^+ , and Li^+). On the other hand, there was a slight decrease in extraction efficiency when 10-fold alkali earth metal ions (Mg^{2+} and Ca^{2+}), Ni^{2+} , and Mn^{2+} were present. This slight decrease was likely due to the high ionic strength of the solution containing alkali earth metal ions, Ni^{2+} and Mn^{2+} , which could lead to a change in adsorption equilibrium. When the solutions contained 10-fold Co^{2+} , Cd^{2+} , Zn^{2+} , and two-fold other rare earth ions (Nd^{3+} and Yb^{3+}), the extraction efficiency for La(III) was obviously affected. The MSCA-12 showed a higher selectivity toward La(III) over alkali metal ions, alkali earth metal ions, transitional metal ions, and other rare earth ions. Moreover, the results also demonstrated that Cl^- , SO_4^{2-} , Ac^- , and NO_3^- did not affect the extraction of La(III) ions.

3.9. Removal of La(III) from the Lake, Groundwater, and Model Wastewater. All of the previously determined optimum parameters were taken into account in the removal of La(III) in real samples. Before the lake and ground waters were used, the contents of metal ions were determined by ICP-AES.

Table 2. Regeneration of Beads by Consecutive Adsorption (A)/Desorption (D) Cycles

	A ₁	D ₁	A ₂	D ₂	A ₃	D ₃	A ₄	D ₄	A ₅	D ₅
[La] _A	0.96 ± 0.3	0	0.92 ± 0.3	0	0.90 ± 0.7	0	0.84 ± 0.9		0.67 ± 0.8	
[La] _D		0.93 ± 0.4		0.90 ± 0.6		0.89 ± 0.5		0.79 ± 0.6		0.64 ± 0.5
[Fe] _R		0.02 ± 0.6		0.03 ± 0.4		0.05 ± 0.7		0.09 ± 0.7		0.102 ± 0.7

Table 3. Extraction Efficiency of MSCA-12 for La(III) in the Presence of Different Salts in Solution^a

ions	add as	WR	RF
La ³⁺			0.968 ± 0.01
Na ⁺	NaCl	100:1	0.964 ± 0.03
K ⁺	KNO ₃	100:1	0.978 ± 0.03
Li ⁺	LiAc	100:1	0.966 ± 0.02
Mg ²⁺	MgCl ₂	10:1	0.913 ± 0.04
Ca ²⁺	CaCl ₂	10:1	0.926 ± 0.06
Ni ²⁺	NiCl ₂	10:1	0.919 ± 0.07
Mn ²⁺	MnCl ₂	10:1	0.942 ± 0.08
Co ²⁺	CoSO ₄	10:1	0.850 ± 0.04
Cd ²⁺	CdCl ₂	10:1	0.855 ± 0.09
Zn ²⁺	ZnSO ₄	10:1	0.802 ± 0.04
Yb ³⁺	YbCl ₃	2:1	0.834 ± 0.03
Nd ³⁺	NdCl ₃	2:1	0.844 ± 0.09

^aWR: weight ratio of metal and La(III) ion; RF: removal fraction.

The results are shown in Table 4. The recovery fraction of La(III) in lake water, groundwater, and artificial wastewater

Table 4. Removal of La(III) in Water Samples by the Proposed Sorbent

sample ^a	measured value (ppm)	added La (mg)	found La (mg)	RSDf	RF
lake water	<0.01	0.17	0.168	0.028	0.988
ground water	0.01	0.17	0.159	0.032	0.935
artificial wastewater	5.20		0.65	0.041	0.903

^aBased on values obtained on triplicate analysis.

were (0.988 ± 0.028), (0.935 ± 0.032), and (0.903 ± 0.041), respectively. The recoveries in all samples are remarkably high. This indicates the high selectivity of the MSCA-12 toward the La(III) ion. Other metal ions as well as other substances present in the sample could probably not compete with La(III) ion in the adsorption process.

4. CONCLUSIONS

The results obtained from this study clearly revealed that superparamagnetic nanosorbent coated by the saponified *sec*-octylphenoxy acetic acid could be used for the selective removal of La(III) from aqueous solution. The extraction efficiency was improved by saponification of extractant and strongly influenced by pH, contact time, ionic strength, interference ions, and metal ion concentration. The optimal condition for removal was equilibrium aqueous pH 7.0 and a contact time of 60 min. The Langmuir model fit the experimental data well with the maximum extraction capacity of 22.0 mg·g⁻¹. The sorbent could be repeatedly used three times and regenerated without significant loss in their binding affinities. The proposed MSCA-12 was applicable for the removal of trace La(III) ion in lake water, groundwater, and artificial wastewater with a high recovery fraction range from 0.988 to 0.903.

AUTHOR INFORMATION

Corresponding Author

*Tel.: +86-021-65982287. Fax: +86-021-65981097. E-mail address: wudongbei@tongji.edu.cn.

Funding

The present work has been carried out under the financial support of the National Natural Science Foundation of China (40802064, 20706045, and 21001085), Innovation Program of Shanghai Municipal Education Commission (12ZZ032), Kwang-Hua Fund for College of Civil Engineering, Tongji University and Shanghai Pujiang Program (No. 11PJ1409500), and Fundamental Research Funds for the Central Universities (No. 1380219106).

REFERENCES

- (1) Sert, Ş.; Kütahyalı, C.; Zeynep, T. S. Biosorption of lanthanum and cerium from aqueous solutions by *Platanus orientalis* leaf powder. *Hydrometallurgy* **2008**, *90*, 13–18.
- (2) Diniz, V.; Volesky, B. Effect of counterions on lanthanum biosorption by *Sargassum polycystum*. *Water Res.* **2005**, *39*, 2229–2236.
- (3) Palyska, W.; Chmielewski, A. G. Solvent Extraction and Emulsion Separation in Magnetic Fields. *Sep. Sci. Technol.* **1993**, *28*, 127–138.
- (4) Ashtari, P.; Wang, K. M.; Yang, X. H.; Huang, S. H.; Yamini, Y. Novel separation and preconcentration of trace amounts of copper(II) in water samples based on neocuproine modified magnetic microparticles. *Anal. Chim. Acta* **2005**, *550*, 18–23.
- (5) Arafat, H. A.; Aase, S. B.; Bakel, A. J.; Bowers, D. L.; Gelis, A. V.; Regalbut, M. C.; Vandegrift, G. F. The application of in situ formed mixed iron oxides in the removal of strontium and actinides from nuclear tank waste. *AIChE J.* **2010**, *56*, 2012–2020.
- (6) Luis, N.; Michael, D. K. Transuranic separation using organophosphorus extractants adsorbed onto superparamagnetic carriers. *J. Magn. Magn. Mater.* **1999**, *194*, 102–107.
- (7) Ozcan, F.; Ersoz, M.; Yilmaz, M. Preparation and application of calix4arene-grafted magnetite nanoparticles for removal of dichromate anions. *Mater. Sci. Eng. C* **2009**, *29*, 2378–2383.
- (8) Shaibu, B. S.; Reddy, M. L. P.; Bhattacharyya, A.; Manchanda, V. K. Evaluation of Cyanex 923-coated magnetic particles for the extraction and separation of lanthanides and actinides from nuclear waste streams. *J. Magn. Magn. Mater.* **2006**, *301*, 312–318.
- (9) Buchholz, B.; Tuazon, H. E.; Kaminski, M. D.; Aase, S. B.; Nunez, L.; Vandegrift, G. F. Optimizing the coating process of organic actinide extractants on magnetically assisted chemical separation particles. *Sep. Purif. Technol.* **1997**, *11*, 211–218.
- (10) Li, W.; Wang, X. L.; Meng, S. L.; Li, D. Q.; Xiong, Y. Extraction and separation of yttrium from the rare earths with *sec*-octylphenoxy acetic acid in chloride media. *Sep. Purif. Technol.* **2007**, *54*, 164–169.
- (11) Wang, Y. G.; Meng, S. L.; Li, D. Q.; Guan, L. Interfacial activity of CA-100 and extraction kinetics of yttrium. *Solvent Extr. Ion Exch.* **2003**, *21* (4), 559–571.
- (12) Wu, D. B.; Zhang, L.; Zhu, B. H.; Yang, Y. H. Adsorption and selective separation of neodymium with magnetic alginate microcapsules containing extractant 2-ethylhexyl phosphonic acid mono-2-ethylhexyl ester. *J. Chem. Eng. Data* **2011**, *56*, 2280–2289.
- (13) Wu, D. B.; Zhao, J.; Zhang, L.; Wu, Q. S.; Yang, Y. H. Lanthanum adsorption using iron oxide loaded calcium alginate beads. *Hydrometallurgy* **2010**, *101*, 76–83.
- (14) Jainae, K.; Sanuwong, K.; Nuangjamnong, J.; Sukpirom, N.; Unob, F. Extraction and recovery of precious metal ions in wastewater by polystyrene-coated magnetic particles functionalized with 2-(3-(2-aminoethylthio) propylthio) ethanamine. *Chem. Eng. J.* **2010**, *160*, 586–593.
- (15) Yang, T. Z.; Shen, C. M.; Gao, H. J. Highly ordered self-assembly with large area of Fe₃O₄ nanoparticles and the magnetic properties. *J. Phys. Chem. B* **2005**, *109*, 23233–23236.
- (16) Chen, Y. W.; Wang, J. L. Preparation and characterization of magnetic chitosan nanoparticles and its application for Cu(II) removal. *Chem. Eng. J.* **2011**, *168*, 286–292.
- (17) Chen, Y. W.; Wang, J. L. Preparation and characterization of magnetic chitosan nanoparticles and its application for Cu(II) removal. *Chem. Eng. J.* **2011**, *168*, 286–293.

(18) Martell, A. E.; Smith, R. M. *Critically selected stability constants of metal complexes database*: National Institute of Standards and Technology (NIST): Gaithersburg, MD, 2004; Version 8.0.

(19) Wang, Y. G.; Yue, S. T.; Li, D. Q.; Jin, M. J.; Li, C. Z. Solvent extraction of scandium (III), yttrium (III), lanthanides (III) and divalent metal ions with sec-nonylphenoxy acetic acid. *Solvent Extr. Ion. Exch.* **2002**, *20*, 701–716.

(20) Chegrouche, S.; Mellah, A.; Telmoune, S. Removal of lanthanum from aqueous solutions by natural bentonite. *Water Res.* **1997**, *31*, 1733–1737.

(21) El-Sofany, E. A. Removal of lanthanum and gadolinium from nitrate medium using Aliquat-336 impregnated onto Amberlite XAD-4. *J. Hazard. Mater.* **2008**, *153*, 948–954.